JOURNAL OF BACTERIOLOGY, Apr. 1992, p. 2525–2538
0021-9193/92/082525-14$02.00/0

Vol. 174, No. 8

Role of the *rfaG* and *rfaP* Genes in Determining the Lipopolysaccharide Core Structure and Cell Surface Properties of *Escherichia coli* K-12

CRAIG T. PARKER,[1] ANDREW W. KLOSER,[1] CARL A. SCHNAITMAN,[1]* MURRY A. STEIN,[2]†
SUSAN GOTTESMAN,[3] AND BRADFORD W. GIBSON[4]

Department of Microbiology, Arizona State University, Tempe, Arizona 85287[1]; Department of Microbiology, Immunology and Parasitology, Louisiana State University Medical Center, New Orleans, Louisiana 70112[2]; Laboratory of Molecular Biology, National Cancer Institute, Bethesda, Maryland 20892[3]; and Department of Pharmaceutical Chemistry, University of California, San Francisco, California 94143[4]

Received 29 October 1991/Accepted 5 February 1992

Deletions which removed *rfa* genes involved in lipopolysaccharide (LPS) core synthesis were constructed in vitro and inserted into the chromosome by linear transformation. The deletion Δ*rfa1*, which removed *rfaGPBI*, resulted in a truncated LPS core containing two heptose residues but no hexose and a deep rought phenotype including decreased expression of major outer membrane proteins, hypersensitivity to novobiocin, and resistance to phage U3. In addition, Δ*rfa1* resulted in the loss of flagella and pili and a mucoid colony morphology. Measurement of the synthesis of β-galactosidase from a *cps-lacZ* fusion showed that the mucoid phenotype was due to *rcsC*-dependent induction of colanic acid capsular polysaccharide synthesis. Complementation of Δ*rfa1* with *rfaG*$^+$ DNA fragments resulted in a larger core and restored the synthesis of flagella and pili but did not reverse the deep rough phenotype or the induction of *cps-lacZ*, while complementation with a fragment carrying only *rfaP*$^+$ reversed the deep rough phenotype but not the loss of flagella and pili. A longer deletion which removed *rfaQGPBIJ* was also constructed, and complementation studies with this deletion showed that the product of *rfaQ* was not required for the functions of *rfaG* and *rfaP*. Thus, the function of *rfaQ* remains unknown. Tandem mass spectrometric analysis of LPS core oligosaccharides from complemented Δ*rfa1* strains indicated that *rfaP*$^+$ was necessary for the addition of either phosphoryl (P) or pyrophosphorylethanolamine (PPEA) substituents to the heptose I residue, as well as for the partial branch substitution of heptose II by heptose III. The substitution of heptose II is independent of the type of P substituent present on heptose I, and this results in four different core structures. A model is presented which relates the deep rough phenotype to the loss of heptose-linked P and PPEA.

The outer membrane of wild-type *Escherichia coli* and *Salmonella typhimurium* acts as a permeability barrier to hydrophobic compounds, providing these strains resistance to hydrophobic antibiotics, detergents, and hydrophobic dyes (35). The asymetric distribution of the lipid components phospholipid and lipopolysaccharide (LPS) across the outer membrane bilayer has been implicated in providing this property, since in wild-type strains LPS is distributed almost entirely in the outer leaflet of the bilayer where it must interact with the environment, while phospholipid is confined to the inner leaflet where it is protected (34, 35). The LPS of enteric bacteria is composed of the glucosamine disaccharide-based lipid A, to which is attached an oligosaccharide core; additionally, in smooth strains about half of the core molecules are substituted by a long, polymeric O antigen. The core oligosaccharide, with its many charged substituents, is likely to be involved in the barrier function, and although the assembly of this structure has been studied for over 20 years, the exact nature of its biosynthesis and role in the barrier function have not been completely determined.

Genes of the *rfa* locus, located between *kbl* and *rpmBG* at 81 min on the *E. coli* K-12 chromosome (43), code for the core assembly enzymes. Evidence that the core region has a role in barrier function comes from a subset of *rfa* mutants with a disrupted barrier function which are said to show a deep rough phenotype. This phenotype is highly pleiotropic and not only includes sensitivity to hydrophobic compounds but also a decrease in the expression of outer membrane proteins, an increase in phospholipids and their redistribution to the outer membrane, and an alteration of sensitivity to LPS-specific and some protein-specific bacteriophage (30, 35, 46). In *S. typhimurium*, strains with mutations in genes encoding functions for heptose transfer (*rfaC*, *-D*, *-E*, and *-F*), glucose transfer to the heptose region (*rfaG*), and decoration of the heptose region (*rfaP*) have been reported to exhibit this phenotype, while strains with mutations in *rfaB*, *-I*, *-J*, *-K*, and *-L*, which are genes encoding functions involved in distal core assembly, do not and are simply termed rough mutants because of their inability to add distal sugars or *O*-polysaccharide (30).

To determine more accurately the cause of the deep rough phenotype as well as the nature of the assembly of the distal core, we have constructed and characterized deletion mutations in the hexose region of the *rfa* locus which cause the deep rough phenotype and we have used various DNA fragments from this region to complement these mutations. This follows our previous study (2) in which complementation of Tn*10* insertion mutants suggested involvement of *rfaG* and *rfaP* in the deep rough phenotype and indicated that genes of the hexose region were organized into a complex operon. Complementation of a deletion can better

* Corresponding author.
† Present address: Department of Pharmaceutical Sciences, College of Pharmacy, Idaho State University, Pocatello, ID 83209.

define the functions of these genes, since it avoids questions raised by incomplete genetic polarity.

During the course of studies on these deletion mutants, we observed several phenotypes not always reported as deep rough characteristics, including cell elongation, loss of pili and flagella, and *rcsC*-dependent induction of capsular polysaccharide synthesis. From the complementation analysis, we demonstrate more precisely the roles of *rfaG* and *rfaP* in the various aspects of the deep rough phenotype and show some of the functions of other genes in the hexose region of *rfa*.

MATERIALS AND METHODS

Strains and genetic techniques. Strain CS180 (P1700 of P. Reeves [3]) was used as the background strain unless otherwise noted. This strain, a derivative of AB1133, was originally constructed for the selection of phage-resistant mutants and carries a *his*-linked *non* mutation. However, as described in this study, this *non* mutation does not completely suppress capsule formation. CS1031 (3) is like CS180 except *rfaP ompA*. Plasmid pHP45 carrying a chloramphenicol-resistant (Cm^r) Ω cassette (13) was obtained from J. Frey. *S. typhimurium* SL4807 (*rfaB707*) was obtained from K. Sanderson, and plasmid DNA isolated from *E. coli* K-12 was introduced into this strain by electroporation as previously described (36).

Transduction with P1 was performed as described by Miller (31). Since strains carrying deletion mutations with a deep rough phenotype became partially resistant to P1 because of the formation of capsule, strains used as P1 donors for transfer of these mutations were constructed in a *cps-5*::Tn*10* (50) derivative of CS180, which substantially improved growth of P1 on these strains. Mutations made on plasmids in vitro were crossed onto the chromosome by transforming the *recBC sbcB* strain VJS803 and *rfaP*::Tn*10* or *cps-5*::Tn*10* derivatives of that strain with linear DNA (52).

Unless otherwise stated, all cultures were grown on LB broth or agar (31). Swarm plates were prepared as described by Ingham et al. (22).

Analysis of *cps-lacZ* fusions. Isogenic strains carrying the *cpsB10-lacZ* fusion were constructed from SG20781 (*lon*$^+$ *cpsB10-lac*) and SG20780 (*lon-510 cpsB10-lac*) (4). The Δ*rfa1*::ΩCm^r and *rcsC10*::Kan mutations were introduced by P1 transduction. The *rcsC10*::Kan mutation is an insertion early in *rcsC* (4). It was transferred to the chromosome by linear transformation (52) and subsequently moved from strain to strain by P1 transduction. For transfer of the Δ*rfa1* mutation, Cm^r mutations were selected with chloramphenicol (15 μg/ml), and it was confirmed that these had acquired sensitivity to bile salts. The *rcsC* allele was selected with kanamycin (30 μg/ml). Strains were constructed either by introduction of the *rfa* allele first followed by introduction of the *rcsC* allele or by introduction in the reverse order, and in both sets of strains the colors of the colonies on LB containing X-Gal (5-bromo-4-chloro-3-indolyl-β-D-galactopyranoside) were in complete agreement. Cells were grown in glucose-Casamino Acids-M63 medium (45), and samples were taken periodically and assayed for β-galactosidase activity as described by Miller (31).

Electron microscopy. Cells growing in LB were seeded at different densities into 1-ml aliquots of LB in 24-well tissue culture plates and grown with agitation at various temperatures. The cells were allowed to grow until log phase and were then processed as follows. A Formvar-coated 400 mesh grid was transferred sequentially to wells containing the culture, water, and 1% uranyl acetate and was air dried on filter paper. Grids were examined at 60 kV with a Phillips EM 200 microscope.

Gel electrophoresis. All cultures for analysis of protein or LPS by gel electrophoresis were grown to the same culture density. Outer membrane proteins were analyzed as described previously (2), and gel loadings were normalized so that each sample represented the same number of cells. For analysis of LPS, proteinase K digests of outer membrane fractions were separated on 18% polyacrylamide gels using a sodium dodecyl sulfate (SDS)-tricine buffer system and visualized by silver staining as described previously (39).

Isolation and purification of LPS and oligosaccharides. LPS was isolated by a modification (2) of the phenol-chloroform-petroleum ether procedure of Galanos et al. (14) from 12-liter cultures grown to late log phase at 30°C. The oligosaccharide fraction was isolated after hydrolysis of the LPS in 1% acetic acid for 90 min exactly as described for preparation B by Gibson et al. (15). This involved chromatography on Sephadex G-50 in pyridinium acetate buffer (pH 4.3), after which the included volume fractions were pooled, lyophilized, and rechromatographed on a Bio-Gel P-4 column (1.5 by 50 cm; fine mesh) in 0.1 M acetic acid. Fractions of 1 ml were assayed for sugar by the phenol-sulfuric acid method (11), and fractions of interest were pooled, lyophilized, redissolved in deionized water, and lyophilized again. Pooled samples were assayed for 3-deoxy-D-*manno*-octulosonic acid (KDO) by the thiobarbituric acid (TBA) assay (26), and absorption spectra of the phenol-sulfuric acid products were compared with those obtained with glucose, KDO, and D-*glycero*-D-*gulo*-heptose (Aldrich Chemical Co., Milwaukee, Wis.) as standards.

Mass spectrometry. The oligosaccharide fractions from Bio-Gel P4 were dissolved in H_2O, and aliquots (about 0.5 μl out of 25 μl) were transferred to a stainless steel probe tip to which had been added approximately 1 μl of a glycerol-thioglycerol (2:1) matrix. Samples were analyzed with a Kratos MS-50 double-focusing mass spectrometer operating at a mass resolution of 1,500 to 2,500 (m/vm, 10% valley). A Cs^+ ion primary beam of 10 keV was used to sputter and ionize the samples with secondary ions accelerated at 6 kV (12). Scans were acquired at 300 s/decade (*m/z* 2,000 to 300) and recorded on a Gould electrostatic recorder. Ultramark 1621 was used to manually calibrate spectra to an accuracy of better than ±0.2 Da. In some samples, salt contamination led to the formation of various sodium and potassium adducts which complicated the spectra, and to eliminate these effects the Bio-Gel fractions were dissolved in 100 μl of 50 mM pyridinium-acetate buffer, pH 5.2, and chromatographed over two TSK-125 Bio-Sil columns (600 by 7.5 mm) connected in series. Detection was by refractive index, using a Knauer RI detector. The total oligosaccharide fractions were pooled and dried and then dissolved in water and applied to the probe as described above. For these samples, a Kratos Concept II HH mass spectrometer was used with postacceleration detection after MS-1 at a scan rate of 30 s/decade (*m/z* 2,000 to 300). Scans were averaged, and mass calibration was performed via a Mach 3 data system with an external CsI calibrant. Possible compositions of the oligosaccharides were determined from their mass spectrometrically determined molecular weights, using a locally developed computer program (20).

Tandem mass spectrometry (MS/MS) analysis. MS/MS spectra were obtained on a four-sector Kratos Concept II HH mass spectrometer with an optically coupled diode array

detector on MS-2 as described elsewhere (37, 51). The spectra were acquired in the negative mode, and a Cs^+ primary beam energy of 18 keV was used to sputter and ionize the oligosaccharides. The C-12 components of the deprotonated molecular ions, $(M-H)^-$, were selected in MS-1, passed through to the helium collision cell floated at 2 keV, and pressure adjusted to attenuate the parent molecular ion by approximately 65%. The daughter ions were separated in MS-2 by using a magnet jump with successive 4% mass windows and a constant B/E ratio. Daughter ions were detected on a 1-in. (ca. 3 cm) optically coupled diode array detector, and masses were assigned automatically by a Kratos Mach 3 data system that used CsI as an external reference for both MS-1 and MS-2 to an overall accuracy of better than ±0.2 Da. The resulting MS/MS spectra were manually interpreted.

RESULTS

Construction and characterization of strains deleted for *rfaG* and *rfaP*. An overview of the *rfa* locus and restriction maps of the deletion mutations and the complementing fragments used in this study is shown in Fig. 1. The deletion Δ*rfa1* involved the removal of an approximately 5.0-kb *Nco*I fragment extending from the 5′ end of *rfaG* through the 3′ end of *rfaI*. This deletion was constructed in plasmid pGEM4rfa8.51 (2), the insert of which is designated in Fig. 1 as SG9.0 (we designate DNA fragments by single-letter abbreviations for the sites at their ends followed by the size in kilobases). After removal of the *Nco*I fragment, the ends were filled in and blunt ended with *Bam*HI linkers, and an Ω Cm^r cassette was inserted into the resulting *Bam*HI site. The plasmid was linearized and transformed into a *recBC sbcB* strain with a mini-Tn*10* insertion (insertion *rfaP81*::Tn*10*) in *rfaP*. Cm^r transformants were screened for U3 resistance ($U3^r$), ampicillin sensitivity, and tetracycline sensitivity, the latter indicating that the chromosomal *rfaP* insertion had been crossed out. When one of the resulting isolates, CS1956, was used as the P1 donor to transduce CS180 to Cm^r, 100% of the transductants also became $U3^r$. One of these transductants, CS1959, was used to characterize the phenotype of the deletion. When a gel of restriction-digested chromosomal DNA from CS1959 was probed with the labeled DNA fragment XA2.1 (Fig. 1), which lies within the deletion, no hybridization was detected by autoradiography, indicating that the deletion had been transferred to the chromosome (data not shown).

In addition to resistance to U3, CS1959 was also sensitive to phage C21 and resistant to K20. The mutant was hypersensitive to novobiocin and did not grow on eosin-methylene blue (EMB) agar or MacConkey agar. When outer membrane proteins were examined by SDS gel electrophoresis, the mutant exhibited a significant reduction in porins and OmpA protein (data not shown), identical to that reported for deep rough insertion mutants (2). It should be noted that one consequence of the reduction in porins (particularly OmpF) was a significant decrease in sensitivity on plates to antibiotics such as ampicillin and kanamycin which require porins for entry. The mutant exhibited partial resistance to phages P1 and λ.

A second, somewhat larger deletion, designated Δ*rfa3*, was constructed from a slightly longer *rfa* insert (Fig. 1) by removal of three contiguous *Hin*dIII fragments extending from the *Hin*dIII site at the 5′ end of *rfaQ* through the *Hin*dIII site in the 3′ end of *rfaJ* and insertion of an Ω Cm^r cassette. The strategy for construction of Δ*rfa3* and its transplacement into the chromosomal *rfa* locus was similar to that described above for Δ*rfa1*. The phenotypic properties of strains carrying Δ*rfa3* were identical in every respect to those of strains carrying Δ*rfa1*, including migration of LPS on gels, acquisition of a mucoid colony appearance (see below), and sensitivity to novobiocin and other hydrophobic compounds. Thus, additional removal of *rfaQ* had no discernible effect. Because the mutations have the same phenotype, the remainder of the studies reported here, except as noted, will deal with Δ*rfa1*.

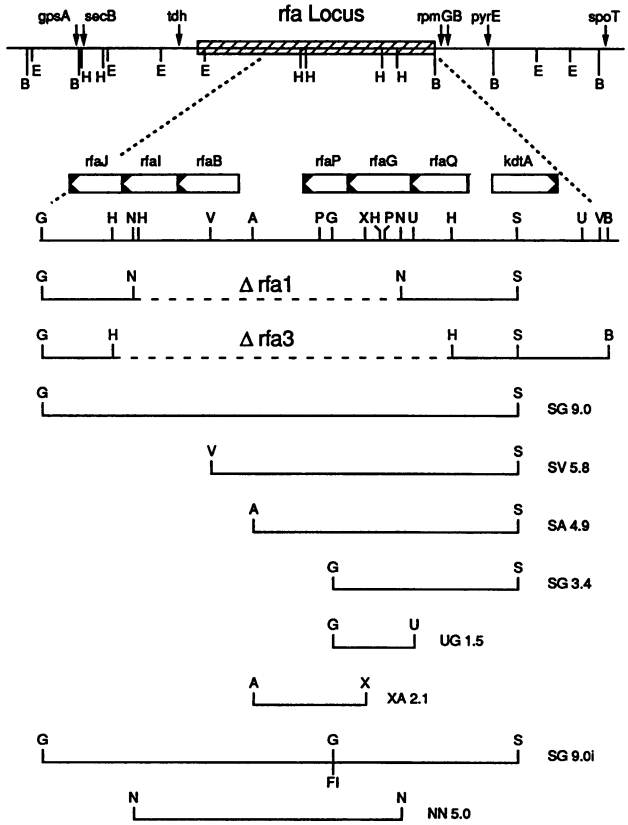

FIG. 1. Restriction fragments from the *kdtA-rfaJ* region of the *rfa* locus. The top portion shows an overview of the *rfa* region at the 81-min region of the *E. coli* K-12 chromosome (43), with the expanded portion showing a partial restriction map of the region from *kdtA* through *rfaJ*. The genes which have been identified from DNA sequence (36, 38) are drawn to scale. The lower portion of the figure shows the various restriction fragments used in this study. Some fragments are the same as those described previously (2) but have been renamed to reflect the true size deduced from the DNA sequence. The dashed portions indicate deletions, and FI indicates an *rfaP* frameshift mutation introduced by filling in and blunt-end ligating a *Bgl*II site. Restriction sites are as follows: A, *Acc*I; B, *Bam*HI; E, *Eco*RI; G, *Bgl*II; H, *Hin*dIII; N, *Nco*I; P, *Pst*I; S, *Sal*I; U, *Pvu*II; V, *Ava*I; and X, *Xba*I.

Capsule induction. Deletion mutants such as CS1959 exhibited characteristics which are not always associated with the deep rough phenotype. One of these was the induction of production of a colanic acid capsular polysaccharide. When freshly transduced into a rfa^+ background, Δ*rfa1* mutants exhibit a characteristic dry, brittle colony morphology we term "crunchy." Upon storage, these colonies acquired a mucoid appearance. The time required for expression of the mucoid phenotype depended upon the temperature of

TABLE 1. Effect of Δ*rfa1* on capsule expression

Genotype[a]	β-Galactosidase[b] (U)					
	32°C		37°C		39°C	
	rcsC$^+$	*rcsC*	*rcsC*$^+$	*rcsC*	*rcsC*$^+$	*rcsC*
lon$^+$ *rfa*$^+$	2.0	2.0	1.9	1.9	1.7	1.8
lon$^+$ Δ*rfa1*	368	1.9	65	1.6	11	1.9
lon-510 rfa$^+$	277	198	159	72	15	4.3
lon-510 Δ*rfa1*	620	151	355	25	107	3.8

[a] All strains are isogenic derivatives of SG20781 (*lon*$^+$) and SG20780 (*lon-510*) carrying a *cpsB10-lac* fusion. The *rcsC10* and Δ*rfa1* mutations were introduced by transduction.

[b] Cells were grown in M63 with glucose and Casamino Acids (45), and enzyme units are as described by Miller (31). All values represent averages of three to five samples taken at different optical densities from logarithmically growing cultures.

growth or storage. At 30°C and below, mucoidy was observed almost immediately, while colonies were not mucoid after growth for 24 h at 37°C. However, storage of such plates at room temperature overnight resulted in all colonies becoming mucoid.

Transduction of a *cps-5*::Tn*10* mutation into CS1959 resulted in a loss of the mucoid phenotype, and introduction of *cps-5*::Tn*10* into strains prior to the introduction of Δ*rfa1* prevented the appearance of the mucoid phenotype. These results indicated that the mucoidy was indeed due to production of colanic acid. The presence of *cps-5*::Tn*10* in strains carrying Δ*rfa1* also eliminated the partial resistance to λ and P1, indicating that the resistance to these phages was due to the production of capsule and was not a primary effect of the *rfa* mutation.

These results suggested that Δ*rfa1* directly affected colanic acid production. To test this hypothesis, the mutation was transferred into strains carrying a *cps-lacZ* operon fusion to permit a quantitative estimation of the expression of capsule biosynthetic genes. Expression of this fusion correlates well with expression of colanic acid (16). As shown in Table 1, in a *lon*$^+$ strain, Δ*rfa1* increased the expression of the *cps-lacZ* fusion dramatically at 32°C. In a *lon* mutant strain which normally expresses capsule at high levels at 32°C but less well at 39°C, the *rfa* deletion increased expression at both temperatures but most noticeably at the nonpermissive temperature.

We were interested in defining the step at which the *rfa* deletion acts to increase capsule expression. A pathway for capsule biosynthesis in which one branch of the pathway uses a membrane protein kinase, RcsC, to signal the RcsB regulator has been proposed (47). It seemed possible that the alteration in the LPS would act by signaling the RcsC membrane protein. We tested this hypothesis by introducing an *rcsC* null mutation into the *cps-lacZ* fusion strains carrying Δ*rfa1*. In both *lon*$^+$ and *lon* hosts, the *rcsC* insertion mutation abolished the *rfa*-dependent increase in *cps* expression. Therefore, the *rfa* mutation acted entirely via the RcsC membrane sensor. Note that the *rcsC* mutation alone had essentially no effect on *cps* expression in a *lon* background. This has been interpreted as being due to an alternative pathway for the induction of capsule synthesis (48). The *rfa* deletion provides the first example of a signal for the regulation of capsule synthesis which is transduced through the RcsC membrane sensor.

Cell elongation and loss of flagella and pili. Ames et al. (1) reported that deep rough mutants lacked flagella and pili.

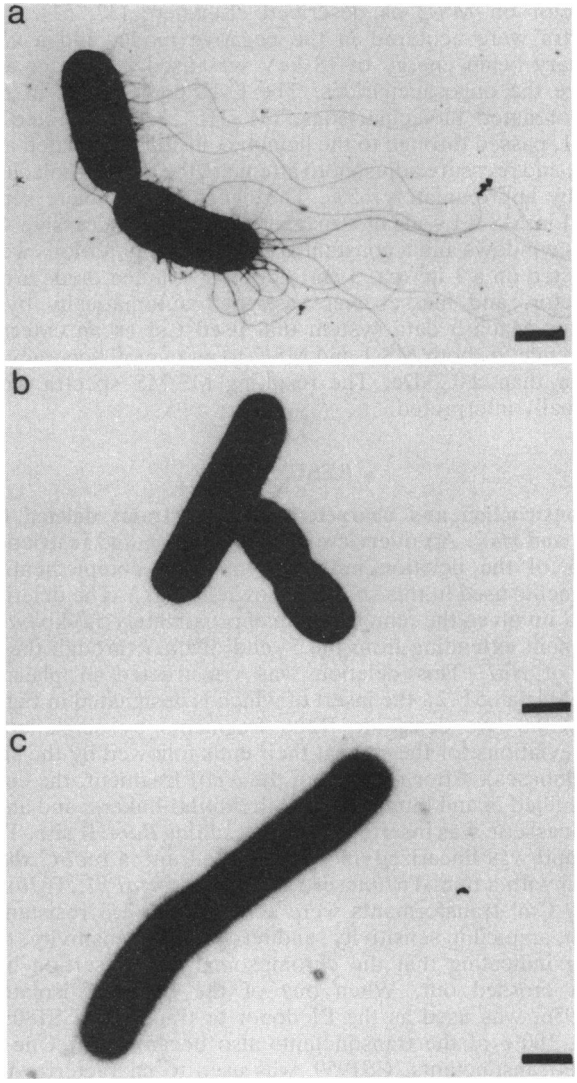

FIG. 2. Loss of flagella and pili due to lack of *rfaG*. (A) Cells of strain CS1977, which is Δ*rfa1*/λSG3.4 (*rfaG*$^+$*P*$^-$). The appearance of these cells is identical to that of the *rfa*$^+$ parent CS180. (B and C) Strain CS1959, which is Δ*rfa1* (*rfaG*$^-$*P*$^-$). The cell in panel C is an example of the filamentation which is sometimes seen with this strain.

This was true also for strains carrying Δ*rfa1*. Under phase-contrast microscopy, individual cells were nonmotile, and the mutant showed no motility on swarm plates. As seen in Fig. 2, electron microscopy indicated that the mutant cells lacked both flagella and pili.

The mutant often grew as filaments, and this was independent of the presence of *cps* mutations. In some experiments, this filamentation appeared to be enhanced by growth at temperatures below 37°C and cultures exhibited a cold-sensitive growth phenotype. Conversely, cultures formed fewer filaments and more cells of normal length when grown at 42°C. The poor reproducibility of these results suggests that this growth phenotype is under control of other factors besides temperature. The Δ*rfa1* mutants grew well at 42°C.

Single-copy complementation. Single-copy complementation was performed by transducing Δ*rfa1* into strains lysogenic for λgt4.0 carrying the *rfa* restriction fragments described in Fig. 1. The phenotypes resulting from this

TABLE 2. Single-copy complementation of Δ*rfaI* by *rfa* restriction fragments cloned into λ

Genotype[a]	Phenotype					
	Phage U3	Phage K20	Novobiocin	Growth on EMB	Outer membrane proteins[b]	Motility
rfa$^+$ (CS180)	S[c]	S	R[d]	+	+	+
rfaQ20::Tn*10*[e]	R	R	S	−	DR	−
Δ*rfaI*	R	R	S	−	DR	−
Δ*rfaI*/λSG3.4 (*rfaG*$^+$)	R	R	S	−	DR	+
Δ*rfaI*/λSA4.9 (*rfaG*$^+$*P*$^+$)	S	S	R	+	+	+
Δ*rfaI*/λSV5.8 (*rfaG*$^+$*P*$^+$)	S	S	R	+	+	+
Δ*rfaI*/λSG9.0 (*rfaG*$^+$*P*$^+$*B*$^+$*I*$^+$*J*$^+$)	S	S	R	+	+	+

[a] Restriction fragments cloned into λ are as in Fig. 1.
[b] A plus sign indicates wild-type outer membrane profile, and DR indicates a reduction in porins and OmpA proteins characteristic of deep rough mutants (2).
[c] S, sensitive.
[d] R, resistant.
[e] This mini-Tn*10* insertion was previously designated *rfa-2* (2).

complementation are shown in Table 2. The defect in the formation of flagella and pili was fully complemented by λSG3.4 which supplied *rfaG*$^+$ (Fig. 2), although the complemented strain retained all of the other characteristics of the deep rough phenotype. This indicates that the loss of flagella and pili is due to the loss of *rfaG* activity and is independent of the deep rough phenotype. However, the induction of capsule expression by Δ*rfaI* was not complemented by *rfaG*$^+$. Lysogenization of SG20781 carrying Δ*rfaI* and the *cpsB10-lac* fusion with a Kan^r-marked derivative of λSG3.4 did not effect the high-level expression of β-galactosidase by this strain, although the electrophoretic mobility of its LPS indicated that it had become *rfaG*$^+$ (data not shown).

Complementation with the shortest fragment tested which supplied both *rfaG* and *rfaP*, SA4.9, restored sensitivity to U3 and K20, a nearly wild-type outer membrane protein profile, and growth on EMB agar. Fragment SA4.9 also eliminated novobiocin hypersensitivity, although the concentration of novobiocin to which cells were resistant continued to increase in strains with larger complementing fragments in proportion to the decrease in LPS gel mobility. These observations confirm previous findings with insertion mutations (2) that the deep rough phenotype can result from the loss of function of a single gene located in the hexose region, identified here as *rfaP*, as well as from the loss of genes such as *rfaC*, *-D*, and *-F* which affect synthesis or attachment of heptose and which are located at the other end of the *rfa* locus (43).

Figure 3 is a comparison of the LPS gel phenotypes of the Δ*rfaI* strains shown in Table 2 to those of Tn*10* insertions in genes *rfaQ*, *-G*, and *-P*. The uncomplemented Δ*rfaI* LPS (lane J) comigrated with the LPS from strains with Tn*10* insertions near the 5′ end of *rfaQ* and in *rfaG* (lanes K and L). As expected, Δ*rfaI* complemented with the *rfaG*$^+$ fragment SG3.5 (lane H) comigrated with LPS from a strain with a Tn*10* insertion in *rfaP* (lane I).

Complementation of Δ*rfaI* with the *rfaG*$^+$*P*$^+$ fragments SA4.9 and SV5.8 resulted in only a slight reduction in LPS migration compared with that of LPS from the deletion complemented only with *rfaG*$^+$ (compare lanes E and G with lane H), despite the other rather large differences in phenotype noted in Table 2. It was also unexpected that the LPS from deletion strains complemented with SA4.9 and SV5.8 would be identical, since the sequence of this region indicates that there is a gene encoding a 36.7-kDa protein between *rfaP* and *rfaB* (Fig. 1) which is present in SV5.8 but interrupted in SA4.9 (38). These aspects of the LPS phenotype are discussed in more detail in the section below dealing with *rfaB*.

There is a striking difference between the complemented phenotypes of Δ*rfaI* and *rfaQ20*::Tn*10*. This is particularly evident in comparing the two mutations complemented by SV5.8 (compare lanes D and E), although it is also seen when both mutations are complemented by SA4.9 (lanes F and G) and SG9.0 (lanes B and C). These results confirm our previous conclusions concerning the incomplete polarity of the *rfaQ20*::Tn*10* insertion. Another interesting aspect of the LPS phenotype is that Δ*rfaI* gave multiple bands only when complemented by SG9.0 (lane C), not when complemented by shorter fragments. This indicates that the production of multiband LPS requires the participation of genes distal to the *Ava*I site at the end of SV4.9. We have recently reached the same conclusion by examining the phenotype of insertions in *rfaI* and *rfaJ* (39).

Identification of *rfaB*. The chemical studies described in the next section below and sensitivity to phage C21 indicated that the LPS produced by Δ*rfaI*/λSA4.9 was of the Rc chemotype, in which the core is truncated after glucose I and lacks the branch galactose (41). As noted above and in Fig. 3, LPS of identical mobility was produced by Δ*rfaI*/λSV5.8, which has a longer insert, indicating that a gene distal to the *Ava*I site between *rfaI* and *rfaP* (Fig. 1) was necessary for the next step in the enlargement of the core. The fact that Rc LPS is produced by *rfaB* mutants of *Salmonella* spp. (53)

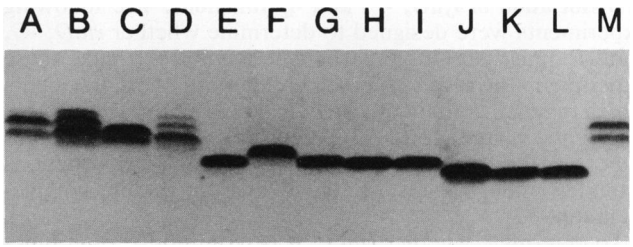

FIG. 3. Silver-stained LPS gel showing single-copy complementation of Δ*rfaI*. Lanes: A and M, LPS from CS180, the *rfa*$^+$ parent; J, Δ*rfaI*; K and L, *rfaQ20*::Tn*10* and *rfaG11*::Tn*10*; F and G, *rfaQ20*::Tn*10*/λSA4.9 and Δ*rfaI*/λSA4.9; H and I, Δ*rfaI*/λSG3.4 and *rfaP81*::Tn*10*; B and C, *rfaQ20*::Tn*10*/λSG9.0 and Δ*rfaI*/λSG9.0; D and E, *rfaQ20*::Tn*10*/λSV5.8 and Δ*rfaI*/λSV5.8. The complementing λ phage are λgt4.0 carrying the fragments shown in Fig. 1, and the Tn*10* insertions are those described previously (2); they have been renamed to reflect the genes in which they are located (36).

and by a Δ*galETK* mutant of *E. coli* which has an RfaB phenotype (42) suggested that the gene distal to the *Ava*I might be *rfaB*.

Genetic mapping in *Salmonella* spp. has yielded the gene order *rfaGBIJ* (25). The fact that *rfaP* is adjacent to and downstream from *rfaG* (36) indicates that *rfaB* should lie between *rfaP* and *rfaI*. Sequencing indicates that there are two contiguous open reading frames in the comparable region of *E. coli* K-12, one of 42,060 Da adjacent to *rfaI* which extends across the *Ava*I site and another of 36,730 Da adjacent to *rfaP* (38, 43). To determine whether either of these was *rfaB*, we examined the ability of pGEM plasmids carrying the *rfa* restriction fragments shown in Fig. 1 to complement the *rfaB* mutation of the *S. typhimurium rfaB707* strain SL4807. The *rfaB* mutation of this strain was completely complemented by a plasmid carrying fragment NN5.0, which includes genes for both open reading frames, as indicated by the restoration of wild-type sensitivity to phages Felix O and P22 and resistance to C21. However, no complementation was observed with a plasmid carrying fragment SV5.8, which carries only the gene for the 36,730-Da open reading frame. This agrees with two other observations which indicate that the gene for the 42,060-Da product is *rfaB*. First, the restriction fragment complementation data for *Salmonella* spp. of Kadam et al. (25), together with the sequences of *rfaI* and *rfaJ* of Carstenius et al. (5), position *rfaB* close to *rfaI*, and, given the similarity of the physical maps of the *rfa* loci of these organisms (43), it is expected that these genes would have a similar location in *E. coli* K-12. Second, a Tn*LacZ* insertion within and near the 5′ end of the coding region of the 42,060-Da protein resulted in the production of type Rc LPS (39). Finally, the 42,060-Da protein shares a region of homology with the products of *rfaG* and *rfaK* (36), proteins which are thought to be sugar transferases (30), while the product of the 36,730-Da open reading frame does not show significant homology to any of the other *rfa* genes which have been sequenced thus far in *E. coli* or *Salmonella* spp.

The product of the 36,730-Da open reading frame is probably the 38-kDa protein previously identified by in vitro transcription-translation (2). Although it is likely that this gene is involved in LPS synthesis, we have not assigned it an *rfa* designation because it shares no homology with other Rfa proteins and there is no direct evidence for *rfa* function. The complementation experiments described above do not rule out the possibility that the products of both the 36,730- and the 42,060-Da open reading frames are required for RfaB function.

Dissociation of *rfaG*, *-P*, and *-Q* functions. The following experiments were designed to determine whether *rfaQ*, *-G*, and *-P* must act in a particular sequence. Since these experiments involved complementation by short fragments which may not contain physiological promoters, we used *rfa* fragments in multicopy pGEM plasmids. Previous studies indicated that fortuitous promoters in such constructions provided enough transcription to give detectable complementation (2).

To determine whether *rfaQ*$^+$ was required for *rfaG* function, a Δ*rfa3* strain (Δ*Q-J*) was transformed with pGEM carrying the *rfaQ*$^-$*G*$^+$ fragment UG1.5. As shown in lane A of Fig. 4, this resulted in LPS which comigrated with the major component of LPS produced by a Δ*galETK* strain (Fig. 4, lane C) which has an Rc chemotype. In addition, the UG1.5 plasmid restored motility on swarm plates to the Δ*rfa3* strain. These results indicate that RfaG function does not require *rfaQ*$^+$. It should be emphasized that this applies only when the *rfaG* product is supplied in *trans*, since the *rfaQ20*::Tn*10* mutation is strongly *cis*-acting (2) and since we have preliminary evidence for other *cis*-acting mutations within the coding region of *rfaQ* which affect the expression of downstream genes.

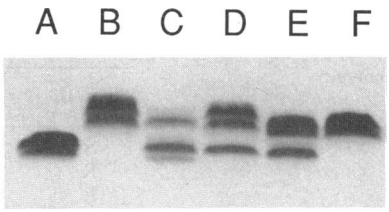

FIG. 4. Silver-stained LPS gel showing complementation of Δ*rfa3* by *rfa* restriction fragments in multicopy plasmids. Restriction fragments are as in Fig. 1. Lanes: A, Δ*rfa3* transformed with pGEM carrying fragment UG1.5 (*rfaG*$^+$); B, CS180 (*rfa*$^+$); C, SA758 (Δ*galETK* [42]); D, CS1031 (*rfaP* point mutant); E, Δ*rfa3* transformed with pGEM carrying SG9.0i; F, Δ*rfa3* transformed with pGEM carrying SG9.0.

In order to ask whether *rfaP* was required for the function of *rfaG* and more distal genes, Δ*rfa3* transformed with a plasmid carrying fragment SG9.0 was compared with the same strain transformed with plasmid carrying fragment SG9.0i, which is identical to SG9.0 except that it has a frameshift mutation near the 5′ end of the *rfaP* coding sequence resulting from a fill-in and blunt-end ligation of the *Bgl*II site. The Δ*rfa3* strain complemented by the SG9.0i plasmid was sensitive to novobiocin and resistant to phage U3, while the same strain complemented by the SG9.0 plasmid was resistant to novobiocin and sensitive to U3, indicating that the SG9.0i fragment was *rfaP*. LPS produced by the two strains is shown in Fig. 4, lanes E and F. The only difference observed in the strain with the *rfaP* plasmid is the appearance of a faster-migrating band which comigrates with Rc LPS. The LPS produced by the Δ*rfa3* strain with the *rfaP* plasmid (lane E) is nearly identical to that produced by a spontaneous *rfaP* mutant of CS180 (lane D). The faster migration of the larger bands seen in lane E is due to the fact that the Ω cassette inserted into the Δ*rfa3* deletion is polar on the distal genes of the operon (*rfaYZK*) which are necessary for core completion (38) and are not present on the plasmid insert. These results indicate that *rfaP* is not required for the action of *rfaG* or for the addition of distal core sugars, although its absence may make completion of the core beyond the Rc stage less efficient than in *rfaP*$^+$ strains. This kind of "leaky" effect on the expression of distal genes has been noted with *rfaP* mutants of *S. typhimurium*, which express some O antigen with a complete core (19).

To test whether *rfaG*$^+$ and *rfaQ*$^+$ were necessary for *rfaP* action, Δ*rfa3* was transformed with a plasmid carrying the XA2.1 insert which carries only *rfaP*. The plasmid restored U3 sensitivity and ability to grow on EMB agar and resulted in a significant increase in resistance to novobiocin. This indicates that *rfaQ*$^+$ and *rfaG*$^+$ are not required for *rfaP* action.

Although novobiocin hypersensitivity is associated primarily with the loss of *rfaP* function, other factors appear to mediate the absolute level of sensitivity to novobiocin in both *rfaP* and *rfaP*$^+$ strains. The sensitivity of Δ*rfa1* strains to novobiocin on plates appeared to be greatest when the mutation was freshly transduced into a new background and to diminish with storage or prolonged manipulation of the culture. We interpret this as the acquisition of unlinked

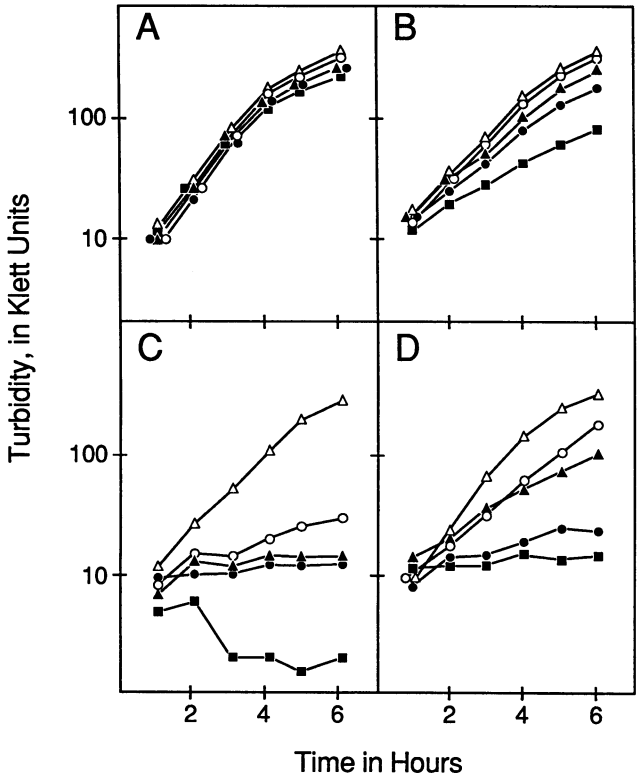

FIG. 5. Effect of *rfaP* and *rfaG* on novobiocin sensitivity. Novobiocin was added at zero time to log-phase cultures growing in LB broth with shaking at 33°C. The final drug concentration was as follows: open triangles, no drug; open circles, 10 μg/ml; closed triangles, 20 μg/ml; closed circles, 40 μg/ml; closed squares, 80 μg/ml. (A) CS180 (*rfa*$^+$); (B) Δ*rfa1* transformed with pGEM carrying fragment XA2.1 (*rfaG*$^-$*P*$^+$); (C) CS1977 (Δ*rfa1*/λSG3.4, *rfaG*$^+$*P*$^-$); (D) CS1959 (Δ*rfa1*, *rfaG*$^-$*P*$^-$).

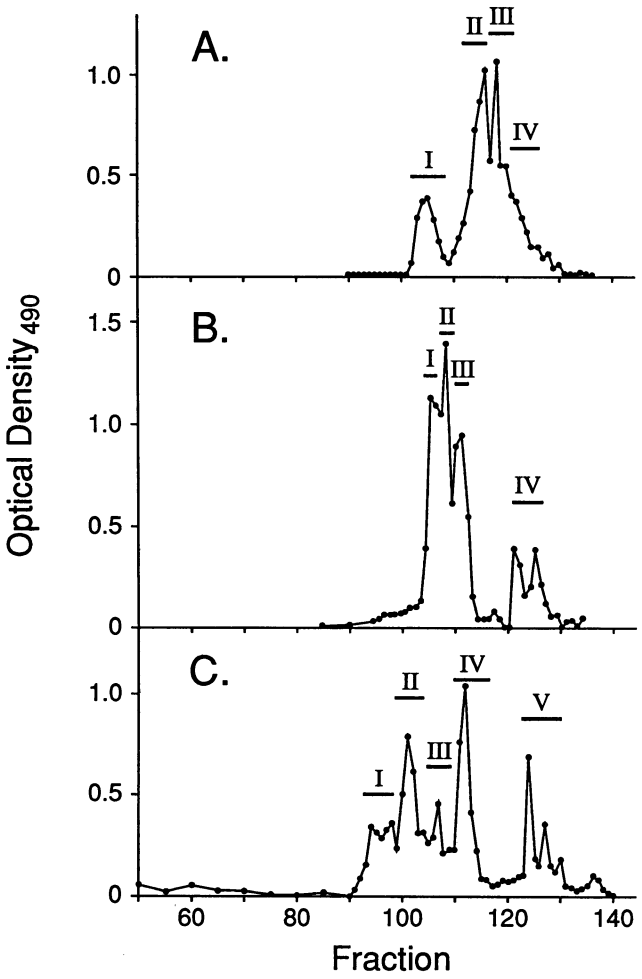

FIG. 6. Gel filtration chromatography of core oligosaccharides. The figure shows the elution of oligosaccharides from a Bio-Gel P4 column as measured by the phenol-sulfuric acid method. The V_0 of the column was at fraction 45, and V_1 was at fraction 140. (A) CS1959 (Δ*rfa1*, *rfaG*$^-$*P*$^-$); (B) CS1977 (Δ*rfa1*/λSG3.4, *rfaG*$^+$*P*$^-$); (C) CS1981 (Δ*rfa1*/λSA4.9, *rfaG*$^+$*P*$^+$). Horizontal bars with roman numerals indicate fractions pooled for mass spectrometric analysis.

suppressor mutations or other regulatory changes. Likely mechanisms include changes in charged substituents added to the lipid A moiety.

The level of sensitivity also appeared to be determined by whether *rfaG*$^+$ was present. To study this in more detail, fresh strains were constructed by transducing Δ*rfa1* into various backgrounds, and these transductants were assayed immediately for novobiocin sensitivity to minimize the accumulation of suppressor mutations. Sensitivity was assayed by adding different levels of the drug to sets of identical liquid cultures, as shown in Fig. 5. The *rfaG*$^-$*P*$^+$ strain exhibited wild-type growth at concentrations of up to 40 μg/ml and grew at about half the wild-type rate at 80 μg/ml. While both the *rfaG*$^+$*P*$^-$ and the *rfaG*$^-$*P*$^-$ strains were almost completely inhibited at 40 μg/ml, the *rfaG*$^+$*P*$^-$ strain was significantly more sensitive than the *rfaG*$^-$*P*$^-$ strain at concentrations of 10 and 20 μg/ml. This is the opposite of what would be expected if loss of *rfaG* contributed to the severity of the deep rough phenotype. One possible explanation is that the loss of *rfaG* triggers compensatory changes in the cell surface which have the effect of reducing the penetration of novobiocin.

Structural analysis of LPS. In order to determine the chemical basis for the deep rough phenotype, we examined the structure of the LPS core oligosaccharides from the Δ*rfa1* strain CS1959 (*rfaG*$^-$*P*$^-$) and the complemented strains CS1977 (Δ*rfa1*/λSG3.4, *rfaG*$^+$*P*$^-$) and CS1981 (Δ*rfa1*/λSA4.9, *rfaG*$^+$*P*$^+$). The linkage of the oligosaccharides to lipid A was cleaved with 1% acetic acid, and after preliminary chromatography on Sephadex G-50 in pyridinium acetate buffer to remove any remaining uncleaved material or lipid A which had failed to sediment, the oligosaccharide fractions were separated on Bio-Gel P4 in 0.1 M acetic acid (Fig. 6). In contrast to the results seen with gel electrophoresis, gel filtration showed significant differences in the apparent sizes of oligosaccharides from *rfaP* and *rfaP*$^+$ strains (Fig. 6B and C). We interpret the discrepancy between the apparent sizes seen by gel filtration and gel electrophoresis as due to an increase in the electrophoretic mobility of *rfaP*$^+$ LPS resulting from the addition of charged substituents, which compensates for the increase in size.

TBA-reactive material was detected in all fractions from all three strains. However, the last fraction from each strain which eluted from the column (fractions IV or V; Fig. 6) appeared to consist of KDO decomposition products, since the ratio of absorbances in the TBA and phenol-sulfuric acid assays was identical to that of authentic KDO. In addition,

TABLE 3. Masses of oligosaccharide $(M-H)^-$ ions derived from LPS

Strain	m/z[a]	Proposed composition[b]	Structure from MS/MS[c]
CS1981 (*rfaG*$^+$*P*$^+$)	**1,178.4**	Hex Hep_3 PPEA KDO	Hex-Hep(Hep)-Hep(PPEA)-KDO
	1,160.4	Hex Hep_3 PPEA KDO*	Hex-Hep(Hep)-Hep(PPEA)-KDO*
	1,055.4	Hex Hep_3 P KDO	Hex-Hep(Hep)-Hep(P)-KDO
	1,037.4	Hex Hep_3 P KDO*	Hex-Hep(Hep)-Hep(P)-KDO*
	986.4	Hex Hep_2 PPEA KDO	Hex-Hep-Hep(PPEA)-KDO
	968.4	Hex Hep_2 PPEA KDO*	Hex-Hep-Hep(PPEA)-KDO*
	863.3	Hex Hep_2 P KDO	Hex-Hep-Hep(P)-KDO
	845.3	Hex Hep_2 P KDO*	Hex-Hep-Hep(P)-KDO*
	711.2		
CS1977 (*rfaG*$^+$*P*$^-$)	1,037.3		
	927.2		
	783.2	Hex Hep_2 KDO	Hex-Hep-Hep-KDO
	765.2	Hex Hep_2 KDO*	Hex-Hep-Hep-KDO*
	603.2	Hep_2 KDO*	Hep-Hep-KDO
CS1959 (*rfaG*$^-$*P*$^-$)[d]	**621.2**	Hep_2 KDO	
	603.2	Hep_2 KDO*	

[a] In all cases, the experimental masses were within ±0.2 Da of the predicted masses based on the proposed compositions. Boldface indicates abundant ions.
[b] Abbreviations: Hex, hexose; Hep, heptose. Blank areas indicate uncertain composition or structure. Asterisks indicate the anhydro form of KDO.
[c] Parentheses indicate branch substituents.
[d] Since the fractions from this strain were analyzed without desalting, only the major abundant ions are shown. Much less abundant ions were seen at *m/z* 685, 707, 805, 823, 861, and 879.

the absorbance spectrum of the phenol-sulfuric acid reaction showed the two peaks characteristic of KDO. This was confirmed by mass spectrographic analysis (data not shown), in which the fragments which were observed in these fractions could be interpreted as being derived from KDO and its breakdown products. These fractions appear to be identical to the PII fraction of Prehm et al. (40), which was proposed to arise from hydrolytic cleavage of branch KDO residues.

A compilation of the larger ions which were detected in significant amounts by liquid secondary ion mass spectrometry (LSIMS) is shown in Table 3. A preliminary composition of each ion was assigned by computerized fitting of the sums of the masses of "generic" components such as the various sugars and of substituents such as pyrophosphorylethanolamine (PPEA) and P which have been reported as components of enteric core oligosaccharides (21, 23, 41). In the samples which were analyzed without desalting, additional ions representing various sodium and potassium adducts, i.e., ions such as $(M+Na-2H)^-$, $(M+K-2H)^-$, $(M+2Na-3H)^-$ etc., were also observed (data not shown). In the cases where it was possible to use tandem (MS/MS) analysis to verify the structures, these are also shown in Table 3.

Figure 7 shows three partial LSIMS spectra, and Fig. 8 and 9 show representative MS/MS spectra of some of the major ions. Spectra A and B of Fig. 7 show LSIMS of two different Bio-Gel fractions from the *rfaP*$^+$*G*$^+$ strain CS1981. The predominant ions in these spectra are pairs of ions of *m/z* 1,160 and 1,178, 1,037 and 1,055, 968 and 986, and 845 and 863. The members of each pair are redundant in that they represent the same parent molecule with either the native or anhydro form of KDO at their reducing terminii. MS/MS analysis (Table 3 and Fig. 9) indicated that these four pairs differed in whether P or PPEA was attached to heptose I and whether a third branch heptose residue was present. The two pairs of ions which contained PPEA were much more abundant in fraction II from the Bio-Gel column, while the two pairs which contained P were more abundant in fraction IV. This indicates that the heterogeneity between P and PPEA substitution was present when the samples were separated on Bio-Gel and was not due to fragmentation during mass spectrometry. The fact that the presence of PPEA had a much more significant effect on elution from Bio-Gel than the presence of an additional heptose residue indicates the bulky hydrodynamic property of the ethanolamine substituent. These spectra also indicate that the four pairs of ions are present in comparable amounts and that the presence or absence of the third heptose substituent attached to heptose II appears to be independent of which kind of phosphoryl substituent is present on heptose I.

The oligosaccharides from the *rfaG*$^+$*P*$^-$ strain CS1977 were very different from those of CS1981 in that the major component observed with LSIMS was a single $(M-H)^-$ ion of *m/z* 765 (Fig. 7C). MS/MS analysis of this ion indicated that much of the apparent homogeneity resulted from the absence of the phosphoryl substituents on heptose I and the absence of partial heptose III substitution of heptose II (Fig. 8).

Figures 8 and 9 illustrates the way MS/MS under collision-inducing conditions was used to elucidate the structures of major ions. Figure 8 shows a relatively simple spectrum arising from the glycosidic and ring cleavages of the unbranched *m/z* 765 oligosaccharide from the *rfaG*$^+$*P*$^-$ strain CS1977. Figure 9 shows the more complicated spectra from $(M-H)^-$ ions observed in oligosaccharides from the *rfaG*$^+$*P*$^+$ strain CS1981. In addition to the types of fragments seen in Fig. 8, spectrum A of Fig. 9 shows abundant low mass ions at *m/z* 79 and 97, corresponding to PO_3^- and $H_2PO_4^-$, respectively. Ions were also seen at high mass which likely arose from the neutral loss of P from the molecular ion, for example, *m/z* 765 $(M-H-HPO_3)^-$ and *m/z* 747 $(M-H-H_3PO_4)^-$. In spectrum B, analogous low mass ions arising from PPEA were observed at *m/z* 79 (PO_3^-), *m/z* 97 ($H_2PO_4^-$), *m/z* 220 (deprotonated PPEA), and *m/z* 202 (PPEA-H_2O), as well as those arising from neutral loss of PPEA (labeled with asterisks) at *m/z* 1,037 $(M-H-PEA)^-$ and *m/z* 1,019 (*m/z* 1,037-H_2O). An additional complexity of spectrum B is due to the third branch heptose which presents more possible glycosidic and ring cleavage cleavage sites identified in the Fig. 9 as α and β.

As was observed with the *rfaG*$^+$*P*$^-$ CS1977, the LSIMS spectra of Bio-Gel fractions from the *rfaG*$^-$*P*$^-$ strain CS1959

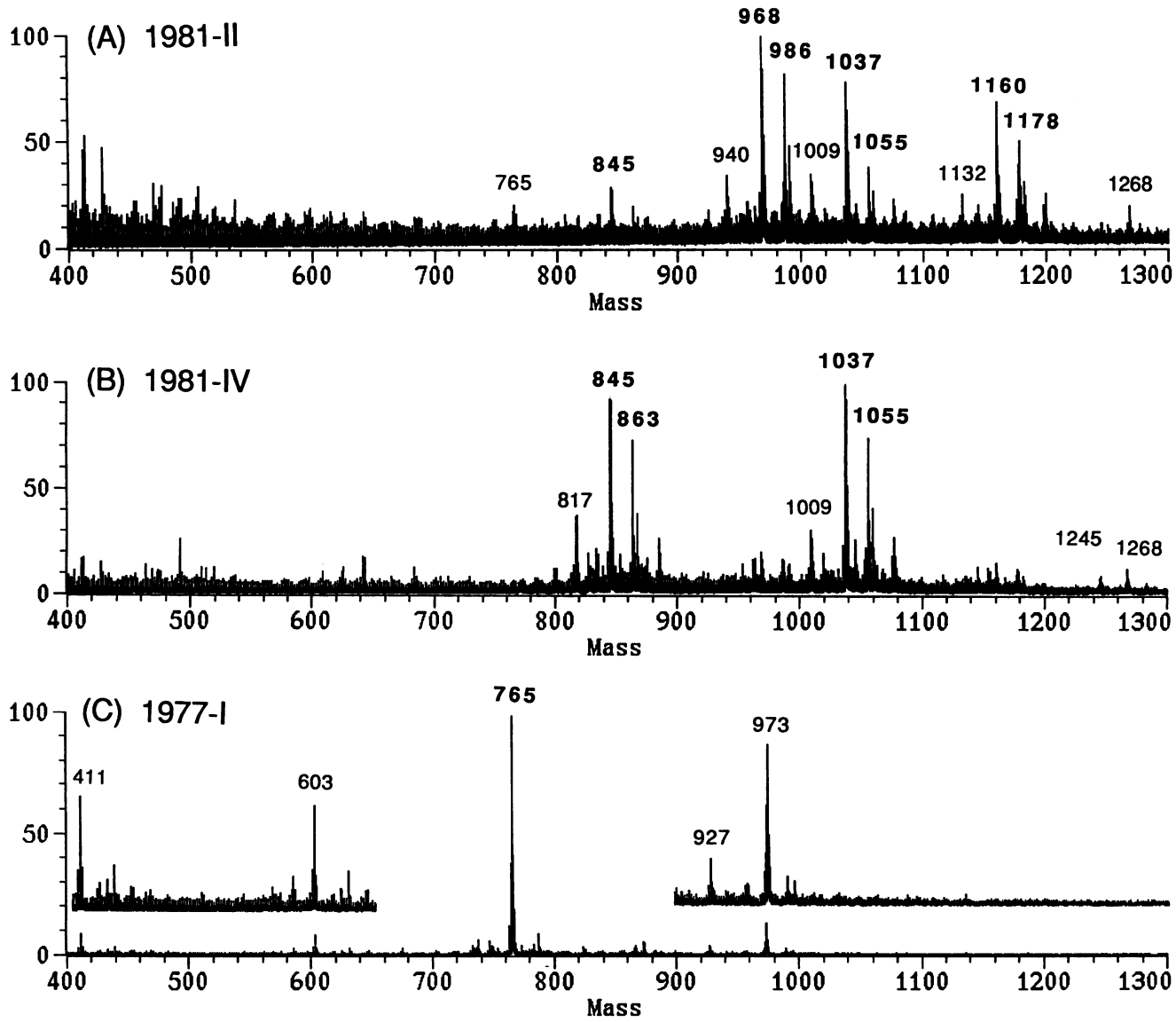

FIG. 7. Partial LSIMS spectra of oligosaccharide Bio-Gel fractions 1981-II (A), 1981-IV (B), and 1977-I (C). The major $(M-H)^-$ ions—i.e., *m/z* 765, 845, 968, 986, 1,037, 1,055, 1,160, and 1,178—are labeled in boldface. Less abundant "satellite ions" 22, 28, and 44 Da larger in mass are seen at lower abundancies and correspond to sodium and potassium adducts. In addition, other high mass ions similar to those observed in other LPS-derived oligosaccharides (15, 24) correspond to matrix-derived adducts such as at *m/z* 973 and 1,245 (+208 Da) and *m/z* 1,269 (+thioglycerol). Accompanying most molecular ions are peaks 28 Da lower in mass which almost certainly arise from loss of CO from the reducing terminal KDO moiety. In panel C, the abundance of the major ion at *m/z* 765 resulted in the appearance of Y-type fragment ions (see Fig. 8) at *m/z* 603 and 411 that correspond to losses of hexose (−162, Y_3) and hexose-hepose (−[162+192], Y_2), respectively, from the nonreducing terminus. Inserts in panel C show a 5× scale expansion.

were relatively simple (spectra not shown). The most abundant ion observed from strain CS1959 was at *m/z* 603 (Table 3), which is consistent with the major ion from CS1977 at *m/z* 765 (Fig. 7C and 8) minus a hexose. This suggests that the structure of the major oligosaccharide of CS1959 is Hep-Hep-KDO. This is in agreement with chemical data indicating that LPS from an *rfaG* insertion mutant lacks glucose (2). The fractions from CS1959 were not characterized by MS/MS.

KDO substituted by phosphorylethanolamine (PEA) was not detected in this study, although it has been reported as a partial substituent in LPS from *rfa*$^+$ *E. coli* K-12 (21) and in type RcP$^-$ LPS from *Salmonella* spp. (21, 28). However, it should be noted that the fractions consisting primarily of free KDO were not characterized extensively and that the cultures from which the LPS was obtained were grown at 30°C. Either of these might have prevented detection of KDO-PEA. KDO-KDO disaccharides which are characteristic mild acid hydrolysis products of cores containing three KDO residues were also not detected, but these were not anticipated, since studies with *Salmonella* spp. indicate that the third KDO residue is added at a late stage of core completion (41).

On the basis of the scheme used for chemotypes in *Salmonella* spp. (41), the data presented above indicate that the LPS of the *rfaP*$^-$*G*$^-$ strain CS1959 is of type Rd1P$^-$, that

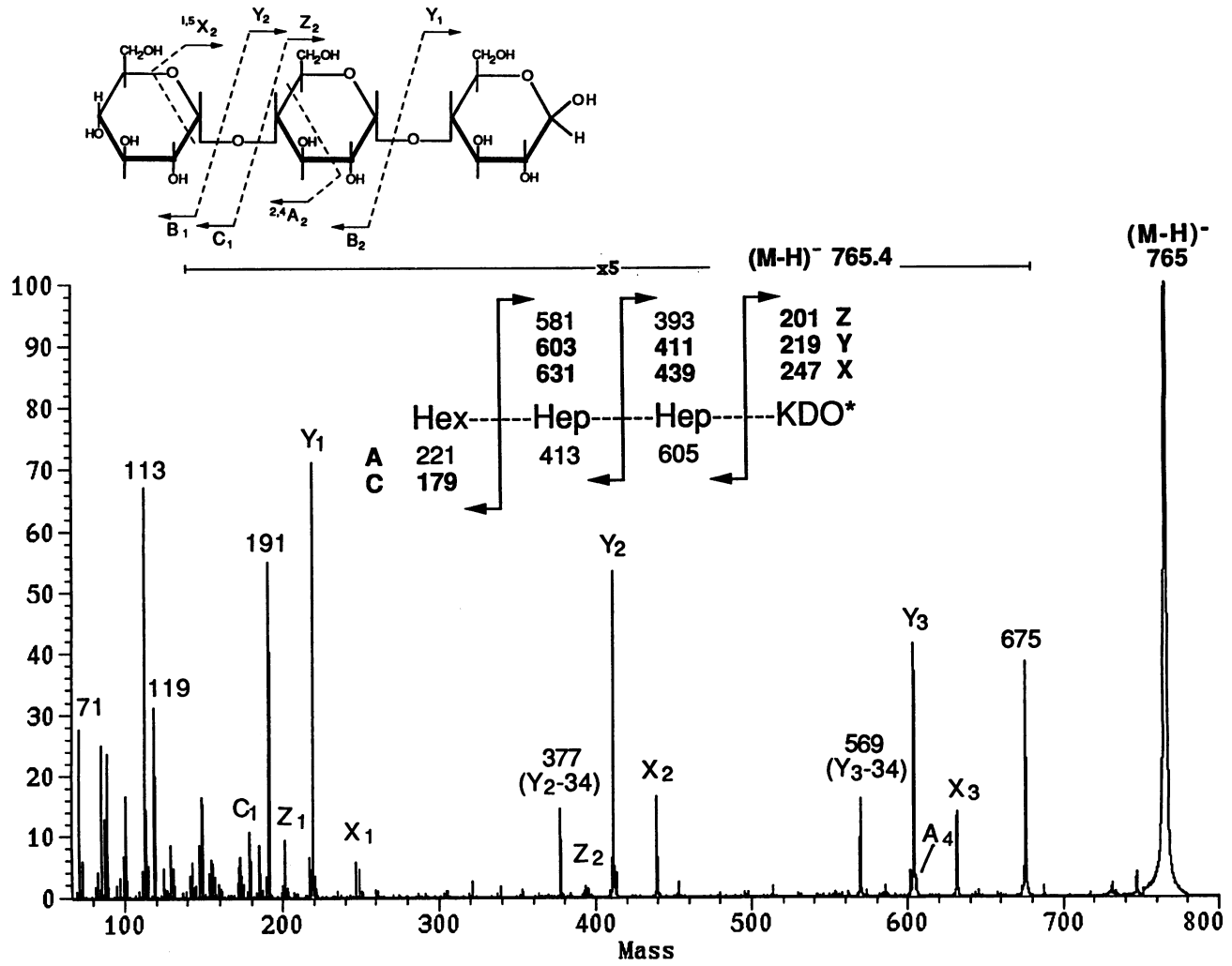

FIG. 8. Tandem collision-inducing (MS/MS) spectrum of $(M-H)^-$ ions at *m/z* 765.4 from CS1977 (Fig. 7C). The insert (top left) shows the carbohydrate fragmentation nomenclature based on that proposed by Domon and Costello (9). The mass difference between fragments of the same type, such as Y_1 and Y_2, define the residue weight, identity, and sequence position. The nominal mass residue masses for the isotopically pure ^{12}C component of common monosaccharides and other moieties in the inner core LPS identified in these studies are 162 Da (hexose), 192 Da (heptose), 202 Da (anhydro KDO), 220 Da (KDO), 80 Da (P), and 203 Da (PPEA). In the case of branched structures, the main branch is defined as α and the secondary branch is defined as β. The origin of the ion at *m/z* 675 is not known, but it is likely to be a nonreducing terminal fragment originating from ring cleavage of KDO.

of the *rfaP*$^-$*G*$^+$ strain CS1977 is of type RcP$^-$, and that of the *rfaP*$^+$*G*$^+$ strain CS1981 is of type RcP$^+$.

DISCUSSION

Effect of *rfa* mutations on expression of flagella and capsules. The lack of flagella observed with Δ*rfaI* appears to be due specifically to the loss of *rfaG* function, suggesting that it results from the absence of glucose I in the LPS core and is not a consequence of the deep rough phenotype. This is in agreement with the results of Komeda et al., who found that *galU* mutants could not synthesize flagella (27). It can be speculated that this is due to a down-regulation of flagellar genes triggered by the change in LPS rather than a problem in the export or assembly of flagellar structures, for two reasons. First, it affects both flagella and pili, which are not known to share a common assembly pathway. Second, Komeda et al. found a decrease in flagellin mRNA in *galU* strains.

The observation that *rfa*-dependent mucoidy is reflected in an *rfa*-dependent increase in *cps-lac* expression demonstrates that it is synthesis of capsule, and not simply its export, which is increased in the *rfa* strain. It is not clear how the *rfa* status of the strain is sensed by RcsC. The RcsC protein has a short periplasmic domain, spans the inner membrane, and has a sizable cytoplasmic domain (47), indicating that it senses something in the periplasm or the cytoplasmic membrane. Sensing may involve intermediates in outer membrane assembly which are thus far unknown.

A number of workers have observed an increase in capsular polysaccharide in *rfa* mutant hosts, and it is thus likely that a variety of mutations which provide early blocks in LPS synthesis generate signals which are ultimately sensed by RcsC. We have observed mucoidy in *rfaP* point mutants

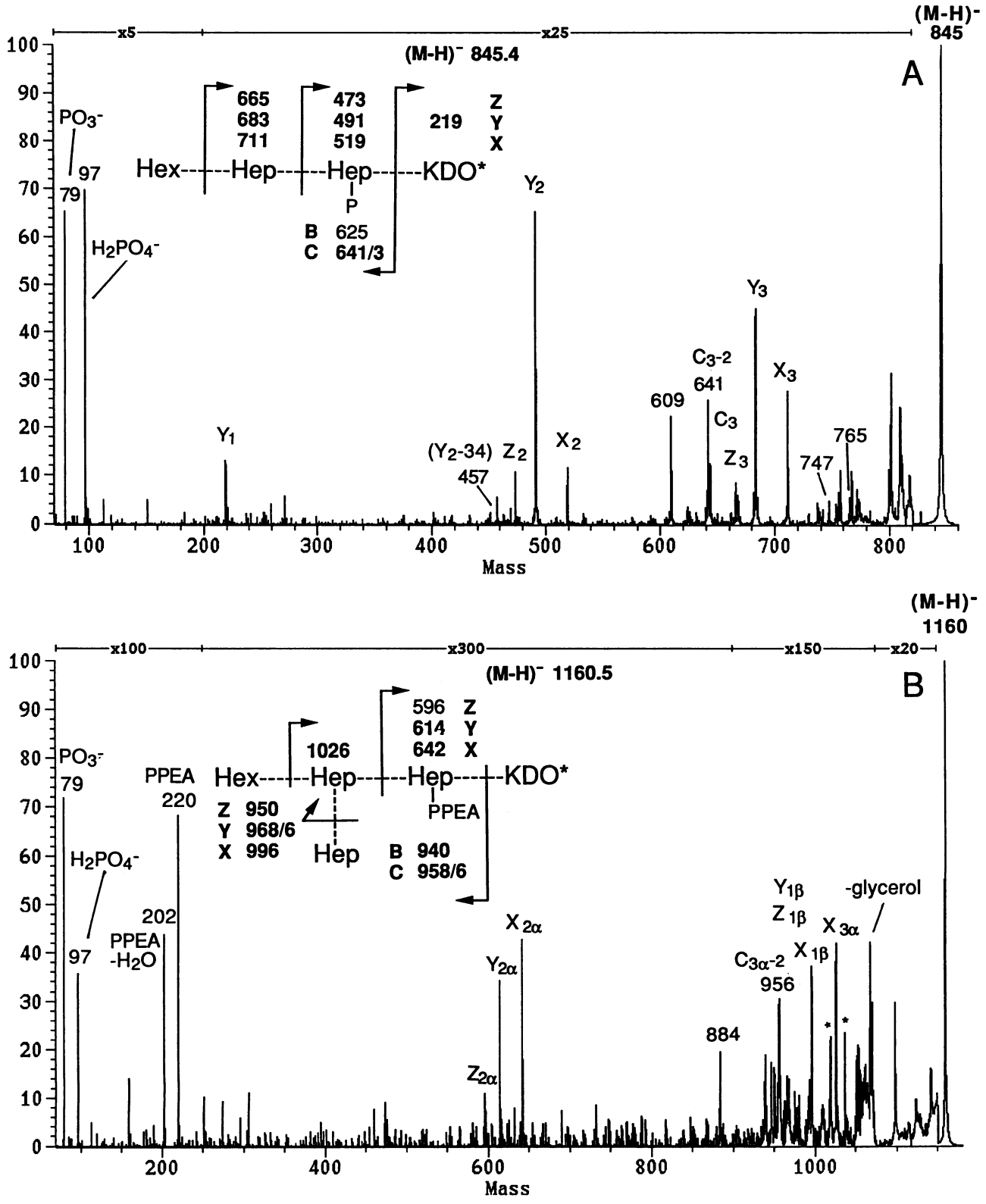

FIG. 9. Tandem collision-inducing (MS/MS) spectrum of $(M-H)^-$ at *m/z* 845.4 (fraction 1981-IV) (A) and *m/z* 1,160.5 (fraction 1981-I) (B). Fragment nomenclature is as in Fig. 8 or as described in the text.

but not in strains with an insertion in *rfaB*. This, together with the observation that the induction of *cps* expression by *Δrfa1* was not complemented by a phage supplying *rfaG*, indicates that *rfaP* mutations are sufficient to induce capsule synthesis. It is not clear whether other mutations affecting LPS which result in expression of capsule do so by interfering with heptose I phosphorylation or by affecting a more general property, such as the physical state of the outer membrane.

The functions of *rfaG* and *rfaP* in determining the LPS inner core structure. The observation that restriction fragments carrying *rfaG*, *-P*, and *-B* from *E. coli* K-12 efficiently complement *Salmonella* mutants with defects in these genes (reference 36 and this study) suggests that the inner core structures on which these gene products act are identical between these organisms. This identity is also supported by mass spectrometric studies on the type RcP^+ core oligosaccharides from the $rfaG^+P^+$ strain CS1981, which indicated that *E. coli* K-12 LPS has structures identical to those reported by Lehmann et al. (28) and Hammerling et al. (17) for RcP^+ oligosaccharides from a *galE* mutant of *Salmonella minnesota*. Thus, it is possible to compare the results of this study with previous work done with *Salmonella* spp. to examine the role these genes play in determining the structure of the LPS inner core and to explore the relationship between LPS structure and the phenotype of deep rough mutants.

Complementation of *rfa* insertions (2) and deletions with restriction fragments carrying known genes indicates that the deep rough phenotype can result from the loss of function of a single gene, *rfaP*. Mass spectrometric analysis of core oligosaccharides from *E. coli* K-12 confirmed studies with *Salmonella* spp. (10, 17, 28, 32) which showed that the most dramatic LPS structural defect in *rfaP* mutants was the loss of P or PPE from the heptose I residue. The additional loss of *rfaG* appears to alter the sensitivity of cells towards novobiocin, as seen in Fig. 7A and B, but this may be an indirect effect of the lack of the glucose I residue. Muhlradt has shown that the transfer of P to the heptose I residue of the core in vitro is more than twice as efficient if the core already contains glucose I (33).

Our results show that the branch heptose III residue is also absent in LPS from an $rfaG^+P^-$ strain, and thus we cannot strictly rule out the lack of heptose III as the cause of the deep rough phenotype. However, the observation that this residue is present as a partial substituent which varies in amount in different strains (17) and the mass spectrometric data which indicate that the heptose I residue carries at least one phosphate in all RcP^+ core molecules argue strongly that it is heptose phosphorylation and not the heptose III residue which is critical with respect to the deep rough phenotype.

A working model to explain the deep rough phenotype. A model for the deep rough phenotype must explain the sensitivity towards detergents and other hydrophobic compounds, the decrease in porins and other major outer membrane proteins, and the increase in phospholipid in the outer leaflet of the outer membrane. The model proposed here is derived from our data and from the data and models regarding outer membrane permeability presented by Nikaido and Vaara (35). We propose that the detergent resistance and the impenetrability towards other hydrophobic compounds exhibited by the outer membrane of enteric bacteria depend upon the presence of at least one set of negatively charged substituents on the LPS core which are positioned so that they can participate in cross-linking of the LPS by divalent metal cations or polyamines. These negatively charged groups might also allow LPS to form intramolecular ionic bonds with positively charged groups on proteins or other LPS molecules. In the chemotype Rc LPS produced by the mutants we have studied, this need is met by phosphate-containing substituents on heptose I. The importance of heptose phosphorylation is supported by the fact that heptose-deficient mutants also exhibit a deep rough phenotype.

There are negatively charged groups in the inner core-lipid A region of LPS which are not affected by deep rough mutations, including phosphoryl and/or pyrophosphoryl groups attached to lipid A (49), PEA attached to some of the branch KDO residues (21, 28), and the carboxyl groups of KDO. However, these either do not participate in divalent cation-mediated cross-linking or do so at very low efficiency, since high levels of divalent cations do not rescue the detergent sensitivity of deep rough mutants. This favors the idea that LPS molecules must pack in the outer membrane in a very specific way so that only some of the charged substituents are capable of being cross-linked by divalent cations. This raises the question of whether P and PPEA, the two charged substituents of heptose I, are both effective in participating in cross-linking.

P and PPEA were found in roughly equal amounts in oligosaccharides from purified RcP^+ LPS. P is likely to be a component of the native LPS and not an artifact due to acid hydrolysis of PPEA. The evidence for this is that acid cleavage sufficient to cleave the pyrophosphoryl group internally would also be expected to attack the pyrophosphoryl-sugar linkage to release PPEA, but we did not observe a significant number of $rfaP^+$ core oligosaccharide molecules in which heptose I was completely dephosphorylated. An identical conclusion was reached by Lehmann et al. (28), who found that acid treatment of KDO-PPEA released only PPEA. Thus, the question is whether the heterogeneity in the substitution of heptose I is due to an inefficient attachment of PEA to P during synthesis or to enzymatic removal of PEA to generate P during maturation of the LPS. If the latter possibility is correct, the bulky ethanolamine moiety might serve as a blocking group to limit cross-linking of the LPS by divalent cations until after its assembly in the outer membrane. There is no direct evidence to support this, but it is attractive as a hypothesis since it provides an explanation for the observation by Levy and Leive (29) that LPS of *E. coli* is synthesized in a form which is resistant to EDTA treatment but is then rapidly converted to a form which can released from the cell by EDTA.

Native porin trimers contain bound LPS (8), and the very specific reduction in major outer membrane proteins such as the porins observed in deep rough mutants could be explained if heptose-PPEA or heptose-P makes up part of the site on LPS which is recognized by newly synthesized outer membrane proteins. Failure to recognize this site might reduce the rate of translocation of proteins to the outer membrane or affect the efficiency of folding or trimerization (44). In deep rough mutants, this could slow the export process, resulting in translational inhibition similar to that which is observed when a defective outer membrane protein is synthesized (6) or when the export machinery is overloaded by overproduction of a single protein (7).

Finally, we propose that the elevated phospholipid content in the outer membrane characteristic of deep rough mutants may result at least in part from a decrease in turnover of phosphatidyl ethanolamine (PE). If the PPEA attached to heptose I arises from the transfer of P and ethanolamine from PE as proposed by Hasin and Kennedy

(18), then LPS synthesis in an *rfa*$^+$ cell must be accompanied by a significant amount of PE turnover. The removal and recycling of diacylglycerol resulting from this turnover might represent an important part of the process of segregating PE and LPS which must occur during the insertion of LPS into the outer leaflet of the outer membrane. The insertion of outer membrane proteins and the cross-linking of LPS by cations may also play a role in the dynamics of exclusion of PE from the outer leaflet (35), and in deep rough mutants it is likely that these processes act synergistically with the reduction in PE turnover to generate the abnormal distribution of PE which is observed.

ACKNOWLEDGMENTS

We thank K. E. Sanderson for strains and helpful discussion.

This research was supported by NSF grant DMB89-96267 (C.A.S.) and Public Health Services grant GM-39087 (C.A.S.) and through the Division of Research Resources (RR-01614) and the NSF (DIR8700-766) for the purchase and support of the tandem mass spectrometer.

REFERENCES

1. **Ames, G. F., E. N. Spudich, and H. Nikaido.** 1974. Protein composition of the outer membrane of *Salmonella typhimurium*: effect of lipopolysaccharide mutations. J. Bacteriol. **117:**406–416.
2. **Austin, E. A., J. F. Graves, L. A. Hite, C. T. Parker, and C. A. Schnaitman.** 1990. Genetic analysis of lipopolysaccharide core biosynthesis by *Escherichia coli* K-12: insertion mutagenesis of the *rfa* locus. J. Bacteriol. **172:**5312–5325.
3. **Beher, M. G., and C. A. Schnaitman.** 1981. Regulation of the OmpA outer membrane protein of *Escherichia coli*. J. Bacteriol. **147:**972–985.4.
4. **Brill, J. A., C. Quinlan-Walshe, and S. Gottesman.** 1988. Fine-structure mapping and identification of two regulators of capsule synthesis in *Escherichia coli* K-12. J. Bacteriol. **170:**2599–2611.
5. **Carstenius, P., J.-I. Flock, and A. Lindberg.** 1990. Nucleotide sequence of *rfaI* and *rfaJ* genes encoding lipopolysaccharide glycosyl transferases from *Salmonella typhimurium*. Nucleic Acids Res. **18:**6128.
6. **Catron, K. M., and C. A. Schnaitman.** 1987. Export of protein in *Escherichia coli*: a novel mutation in *ompC* affects expression of other major outer membrane proteins. J. Bacteriol. **169:**4327–4334.
7. **Click, E. M., G. A. McDonald, and C. A. Schnaitman.** 1988. Translational control of exported proteins that results from OmpC porin overexpression. J. Bacteriol. **170:**2005–2011.
8. **Diedrich, D. L., M. A. Stein, and C. A. Schnaitman.** 1990. Associations of *Escherichia coli* K-12 OmpF trimers with rough and smooth lipopolysaccharides. J. Bacteriol. **172:**5307–5311.
9. **Domon, B., and C. E. Costello.** 1988. A systematic nomenclature for carbohydrate fragmentations in FAB-MS/MS spectra of glycoconjugates. Glycoconjugate J. **5:**397.
10. **Droge, W., E. Ruschmann, O. Lüderitz, and O. Westphal.** 1968. Biochemical studies on lipopolysaccharides of *Salmonella* R mutants. 4. Phosphate groups linked to heptose units and their absence in some R lipopolysaccharides. Eur. J. Biochem. **4:**134–138.
11. **Dubois, M., K. Gilles, J. K. Hamilton, P. A. Rebers, and F. Smith.** 1956. Colorimetric method for determination of sugars and related substances. Anal. Chem. **28:**350–356.
12. **Falick, A. M., G. H. Wang, and F. C. Walls.** 1986. Ion source for liquid matrix secondary ionization mass spectrometry. Anal. Chem. **58:**1308.
13. **Fellay, R., J. Frey, and H. M. Kritsch.** 1987. Interposon mutagenesis of soil and water bacteria: a family of DNA fragments designed for *in vitro* insertional mutagenesis of Gram-negative bacteria. Gene **52:**147–154.
14. **Galanos, C., O. Lüderitz, and O. Westphal.** 1969. A new method for extraction of R lipopolysaccharides. Eur. J. Biochem. **9:**245–249.
15. **Gibson, B. W., J. W. Webb, R. Yamasaki, S. J. Fisher, A. L. Burlingame, R. E. Mandrell, H. Schneider, and J. M. Griffiss.** 1989. Structure and heterogeneity of the oligosaccharides from lipopolysaccharides of *Neisseria gonorrhoeae*. Proc. Natl. Acad. Sci. USA **86:**17–21.
16. **Gottesman, S., P. Trisler, and A. Torres-Cabassa.** 1985. Regulation of capsular polysaccharide in *Escherichia coli* K-12: characterization of three regulatory genes. J. Bacteriol. **162:**1111–1119.
17. **Hämmerling, G., V. Lehmann, and O. Lüderitz.** 1973. Structural studies on the heptose region of *Salmonella* lipopolysaccharides. Eur. J. Biochem. **38:**453–458.
18. **Hasin, M., and E. P. Kennedy.** 1982. Role of phosphatidylethanolamine in the biosynthesis of pyrophosphoethanolamine residues in lipopolysaccharide of *Escherichia coli*. J. Biol. Chem. **257:**12475–12477.
19. **Helander, I. M., M. Vaara, S. Sukupolvi, M. Rhen, S. Saarela, U. Zähringer, and P. H. Mäkelä.** 1989. *rfaP* mutants of *Salmonella typhimurium*. Eur. J. Biochem. **185:**541–546.
20. **Hines, M.** Unpublished data.
21. **Holst, O., E. Rohrscheidt-Andrzejewski, H. Brade, and D. Charon.** 1990. Isolation and characterisation of 3-deoxy-D-*manno*-2-octulopyranosonate 7-(2-aminoethyl phosphate) from the inner core region of *Escherichia coli* K-12 and *Salmonella minnesota* lipopolysaccharides. Carbohydr. Res. **204:**93–102.
22. **Ingam, C., M. Buechner, and J. Adler.** 1990. Effect of outer membrane permeability on chemotaxis in *Escherichia coli*. J. Bacteriol. **172:**3577–3583.
23. **Jansson, P.-E., A. A. Lindberg, B. Lindberg, and R. Wollin.** 1981. Structural studies on the hexose region of the core in lipopolysaccharides from enterobacteriaceae. Eur. J. Biochem. **115:**571–577.
24. **John, C. M., J. M. Griffiss, M. A. Apicella, R. E. Mandrell, and B. W. Gibson.** 1991. The structural basis for pyocin resistance in *Neisseria gonorrhoeae* lipooligosaccharides. J. Biol. Chem. **266:**19301–19311.
25. **Kadam, S. K., A. Rehemtulla, and K. E. Sanderson.** 1985. Cloning of *rfaG*, *B*, *I*, and *J* genes for glycosyltransferase enzymes for synthesis of the lipopolysaccharide core of *Salmonella typhimurium*. J. Bacteriol. **161:**277–284.
26. **Karkhanis, Y. D., J. Y. Zeltner, J. J. Jackson, and D. J. Carlo.** 1978. A new and improved microassay to determine 2-keto-3-deoxyoctonate in lipopolysaccharide of gram-negative bacteria. Anal. Biochem. **85:**595–601.
27. **Komeda, Y., T. Icho, and T. Iino.** 1977. Effects of *galU* mutation on flagellar formation in *Escherichia coli*. J. Bacteriol. **129:**908–915.
28. **Lehmann, V., O. Lüderitz, and O. Westphal.** 1971. The linkage of pyrophosphorylethanolamine to heptose in the core of *Salmonella minnesota* lipopolysaccharides. Eur. J. Biochem. **21:**339–347.
29. **Levy, S. B., and L. Leive.** 1968. An equilibrium between two fractions of lipopolysaccharide in *Escherichia coli*. Proc. Natl. Acad. Sci. USA **61:**1435–1439.
30. **Mäkelä, P. H., and B. A. D. Stocker.** 1984. Genetics of lipopolysaccharide, p. 59–137. *In* E. T. Rietschel (ed.), Handbook of endotoxin, vol. 1. Chemistry of endotoxin. Elsevier, Amsterdam.
31. **Miller, J. H.** 1972. Experiments in molecular genetics. Cold Spring Harbor Laboratory, Cold Spring Harbor, N.Y.
32. **Mühlradt, P. F.** 1969. Biosynthesis of *Salmonella* lipopolysaccharide. The *in vitro* transfer of phosphate to the heptose moiety of the core. Eur. J. Biochem. **11:**241–248.
33. **Mühlradt, P. F.** 1971. Biosynthesis of *Salmonella* lipopolysaccharide. Studies on the transfer of glucose, galactose and phosphate to the core in a cell free system. Eur. J. Biochem. **18:**20–27.
34. **Mühlradt, P. F., and J. R. Golecki.** 1975. Asymmetrical distribution and artifactual reorientation of lipopolysaccharide in the outer membrane bilayer of *Salmonella typhimurium*. Eur. J. Biochem. **51:**343–352.
35. **Nikaido, H., and M. Vaara.** 1985. Molecular basis of bacterial outer membrane permeability. Microbiol. Rev. **49:**1–32.

36. **Parker, C. T., E. Pradel, and C. A. Schnaitman.** 1991. Identification and sequences of the lipopolysaccharide core biosynthetic genes *rfaQ*, *rfaP*, and *rfaG* of *Escherichia coli* K-12. J. Bacteriol. **174:**930–934.
37. **Phillips, N. J., C. M. John, L. G. Reinders, J. M. Griffiss, M. A. Apicella, and B. W. Gibson.** 1990. Structural models for cell surface lipooligosaccharides of *Neisseria gonorrhoeae* and *Haemophilus influenzae*. Biomed. Environ. Mass Spectrom. **19:** 731–745.
38. **Pradel, E., C. T. Parker, and J. D. Klena.** Unpublished data.
39. **Pradel, E., and C. A. Schnaitman.** 1991. Effect of *rfaH* (*sfrB*) and temperature on expression of *rfa* genes of *Escherichia coli* K-12. J. Bacteriol. **173:**6428–6431.
40. **Prehm, P., S. Stirm, B. Jann, and K. Jann.** 1975. Cell-wall lipopolysaccharide from *Escherichia coli* B. Eur. J. Biochem. **56:**41–55.
41. **Rick, P. D.** 1987. Lipopolysaccharide biosynthesis, p. 648–662. *In* F. Neidhardt, J. L. Ingraham, K. B. Low, B. Magasanik, M. Schaechter, and H. E. Umbarger (ed.), *Escherichia coli* and *Salmonella typhimurium*, vol. 1. American Society for Microbiology, Washington, D.C.
42. **Schnaitman, C. A., and E. A. Austin.** 1990. Efficient incorporation of galactose into lipopolysaccharide by *Escherichia coli* K-12 strains with polar *galE* mutations. J. Bacteriol. **172:**1256–1287.
43. **Schnaitman, C. A., C. T. Parker, J. D. Klena, E. L. Pradel, N. B. Pearson, K. E. Sanderson, and P. R. MacLachlan.** 1991. Physical maps of the *rfa* locus of *Escherichia coli* K-12 and *Salmonella typhimurium*. J. Bacteriol. **173:**7410–7411.
44. **Sen, K., and H. Nikaido.** 1991. Lipopolysaccharide structure required for in vivo trimerization of *Escherichia coli* OmpF porin. J. Bacteriol. **173:**926–928.
45. **Silhavy, T. J., M. L. Berman, and L. W. Enquist.** 1984. Experiments with gene fusions. Cold Spring Harbor Laboratory, Cold Spring Harbor, N.Y.
46. **Silverman, J. A., and S. A. Benson.** 1987. Bacteriophage K20 requires both the OmpF porin and lipopolysaccharide for receptor function. J. Bacteriol. **169:**4830–4833.
47. **Stout, V., and S. Gottesman.** 1990. RcsB and RcsC: a two-component regulator of capsule synthesis in *Escherichia coli*. J. Bacteriol. **172:**659–669.
48. **Stout, V., A. Torres-Cabassa, M. R. Maurizi, D. Gutnick, and S. Gottesman.** 1991. RcsA, an unstable positive regulator of capsular polysaccharide synthesis. J. Bacteriol. **173:**1738–1747.
49. **Strain, S. M., I. M. Armitage, L. Anderson, K. Takayama, N. Gureshi, and C. R. H. Raetz.** 1985. Location of polar substituents and fatty acid chains on lipid A precursors from a 3-deoxy-D-*manno*-octulosonic acid-deficient mutant of *Salmonella typhimurium*. J. Biol. Chem. **260:**16089–16098.
50. **Trisler, P., and S. Gottesman.** 1984. *lon* transcriptional regulation of genes necessary for capsular polysaccharide synthesis in *Escherichia coli* K-12. J. Bacteriol. **160:**184–191.
51. **Walls, F. C., M. A. Baldwin, M. A. Falick, B. W. Gibson, B. L. Gillece-Castro, S. Kaur, D. A. Maltby, K. F. Medzihradsky, S. Evans, and A. L. Burlingame.** 1990. Experience with multichannel array detection in tandem mass spectrometric characterization of biopolymers at the picomole level, p. 197–216. *In* J. A. McClosky and A. L. Blurlingame (ed.), Biological mass spectrometry. Elsevier, Amsterdam.
52. **Winans, S. C., S. J. Elledge, J. H. Krueger, and G. C. Walker.** 1985. Site-directed insertion and deletion mutagenesis with cloned fragments in *Escherichia coli*. J. Bacteriol. **161:**1219–1222.
53. **Wollin, R., E. S. Creeger, L. I. Rothfield, B. A. D. Stocker, and A. A. Lindberg.** 1982. *Salmonella typhimurium* mutants defective in UDP-D-galactose:lipopolysaccharide α1,6-D-galactosyltransferase. J. Biol. Chem. **258:**3769–3774.